Analysis of the sign-dependent switching observed in a hybrid aligned nematic cell

S L Cornford[1,2]**, T S Taphouse**[1] **and J R Sambles**

School of Physics, University of Exeter, Exeter, Devon, UK
E-mail: sc261@ex.ac.uk

Abstract. An optical waveguide experiment was used to study the influence of dc electric fields on a hybrid aligned nematic liquid crystal cell. This dc switching differed from ac switching in two ways: first, the equilibrium states depended on the sign of the applied voltage, and second, there was transient activity over long ($\sim$100 ms) timescales. To understand both of these, a numerical model of the cell's dynamics, which included both the Ericksen–Leslie theory and a drift-diffusion model of mobile ions, has been developed. Comparing modelling with observations, we find that the transients are caused by the motion of tiny concentrations of ionic impurities, and that the sign dependence is caused by an asymmetric distribution of surface charge, rather than the flexoelectric effect.

Contents

[1] Current address: HP Labs, Bristol, UK.
[2] Author to whom any correspondence should be addressed.

IOP Institute of Physics ❶DEUTSCHE PHYSIKALISCHE GESELLSCHAFT

1. Introduction

Calamitic nematic liquid crystals are made up of elongated molecules which tend to align with one another, but are otherwise unordered. It is usual to denote the average alignment of these molecules over a small volume by a unit vector $\boldsymbol{n}$, called the director. These materials are commonly utilized in liquid crystal displays (LCDs), built by sandwiching a layer of liquid crystal between glass plates whose surfaces are treated to influence the director adjacent to them. Elastic forces then cause the liquid crystal to adopt a ground state in which the director varies smoothly from one surface to the other. Applying an electric field changes the orientation of the director, allowing the optical properties of the cell to be controlled. In ordinary devices, the director returns to its ground state once the electric field has been removed.

Among recent innovations in LCD technology are bistable nematic devices, in which both a light and a dark state are stable in the absence of an electric field. In the Zenithal Bistable Device (ZBD) [1], a layer of nematic liquid crystal is sandwiched between two transparent substrates. A blazed grating is fabricated onto one substrate and treated to promote homeotropic alignment, where the director is perpendicular to the surface. Two stable alignments occur just beyond the grating: one approximately perpendicular to the cell substrates and the second roughly parallel to them. Another bistable device, the Post-Aligned Bistable Nematic (PABN) device [2], employs an array of micron scale posts to effect a bistable surface. In both designs, the other surface is treated to promote homeotropic alignment. Thus, both the ZBD and the PABN resemble a hybrid aligned nematic (HAN) cell in one state and a vertically aligned nematic (VAN) cell in the other.

These bistable cells can be switched from the HAN state to the VAN state by applying a voltage pulse of one polarity, and back by a pulse of the opposite polarity. So, some mechanism must be responsible for driving the director in a different direction depending on the sign of the field applied across the electrodes. In ordinary liquid crystal devices, the cell is driven from its ground state to an excited state when an ac electric field is applied through a change to the free energy in the bulk. If the dielectric tensor is $\boldsymbol{\epsilon}$, then an electric field $\boldsymbol{E}$ gives rise to a contribution to the free energy density $-\boldsymbol{E}.\boldsymbol{\epsilon}.\boldsymbol{E}/2$ which is always negative and proportional to E^2, and is therefore unchanged by reversing the direction of $\boldsymbol{E}$. While a bistable device could be driven from (say) the HAN state to the VAN state (or vice versa), the opposite cannot be achieved. Instead, some effect dependent on the sign of E must be responsible.

One such sign-dependent effect is the flexoelectric effect [3], where an electric polarization,

$$\boldsymbol{P} = e_s \boldsymbol{n}\boldsymbol{\nabla}.\boldsymbol{n} + e_b \boldsymbol{n} \times \boldsymbol{\nabla} \times \boldsymbol{n}, \tag{1}$$

is induced by curvature strains. Here, we have adopted the convention of Rudquist and Lagerwall [4] in labelling the splay- and bend-flexoelectric coefficients e_s and e_b, respectively, and in choosing the sign of e_b. The flexoelectric contribution to the free energy density, $-\boldsymbol{P}.\boldsymbol{E}/2$, *does* depend upon the sign of E: for a given director profile, reversing the direction of $\boldsymbol{E}$ changes the sign of $-\boldsymbol{P}.\boldsymbol{E}/2$. Since the director profile in a HAN cell is not symmetric about the mid-plane, the total free energy is also sign dependent. Experimental studies that exploit this sign dependence in order to measure $(e_s - e_b)$ include both dc [5]–[7] and low frequency ac [8] techniques. Numerical studies have shown that the flexoelectric effect can indeed cause switching in a bistable device [9], provided that $|e_s - e_b|$ is large enough.

A second sign-dependent effect occurs if charged carriers are bound asymmetrically to the walls, leading to an internal field which may enhance or oppose the applied field. Impurity
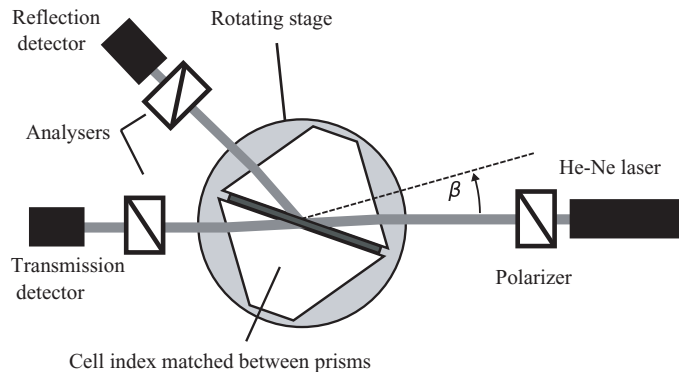
Figure 1. The fully leaky guided mode experiment apparatus. The angle β between the incident beam and the normal to the first prism face is varied, allowing the reflection and transmission coefficients to be measured as a function of β.

molecules in the nematic liquid crystal may decompose into ions, and are either adsorbed onto the cell walls or remain mobile in the bulk liquid crystal [10]–[12]. In the HAN geometry, in steady state, it is difficult to distinguish between such surface polarization and flexoelectricity: previous studies have examined the form of the ground state director profile in order to make the necessary distinction [6, 7]. However, the presence of mobile ions in the cell will reduce the accuracy of such a method.

We use the fully leaky guided mode experiment to study a HAN cell, subjected to dc electric fields. In a previous paper, appreciable dependence upon the sign of E was observed in the cell's steady states [13]. This could be explained equally well by the flexoelectric effect or by bound surface charges. Here, the behaviour of the liquid crystal as it approaches equilibrium is considered. While we see the normal behaviour, namely viscous rotation and the backflow effect, we also see transient features over timescales $\sim$100 ms, far longer than the $\sim$10 ms timescales which are seen in the ac switching of the same cell. To model the experiment, we numerically solve the Ericksen–Leslie equations [14, 15], which adequately describe the ac behaviour, together with a drift-diffusion model of ionic impurities [16, 17]. Ultimately, we find that the form of the transients is consistent with an assumption that the sign-dependent effect is dominated by bound surface charges.

2. Experimental method

The time-resolved fully leaky guided-mode experiment [18, 19] shown in figure 1 is designed to detect changes in the director profile with sub-millisecond resolution. A liquid crystal cell is coated with index matching fluid and set between glass prisms, then the resulting assembly is mounted on a rotating table so that the prism faces are parallel to the laboratory y-axis. The polarizer and analysers are set to select either s- or p-polarized light and the rotating table set to an initial angle β. A time-dependent electric potential, $v_0(t)$, is applied across the cell, and the reflection coefficient and transmission coefficient measured as a function of time. These time-dependent measurements are repeated for a range of angles and for each permutation of polarizer and analyser states. For each time and angle, eight signals R_{pp}, R_{ps}, R_{sp}, R_{ss}, T_{pp}, T_{ps},

T_{sp} and T_{ss} are recorded, where the first subscript denotes the state of the polarizer, and the second subscript denotes the state of the analyser.

It is a simple matter to predict the signals $R_{pp}, \dots T_{ss}$ when the director profile is known, using Berreman's 4×4 matrix method [20]. However, solutions to the corresponding inverse problem— calculation of the director profile given the experimental data—can only be obtained by special techniques [22]. Briefly, we seek a director profile consistent with the experimental data and broadly consistent with, but not constrained to be solutions of, the Ericksen–Leslie equations.

A $3\,\mu$m thick HAN cell filled with Merck ZLI-4788-000 is studied in this paper. This nematic liquid crystal has a negative dielectric anisotropy ϵ_a, so that at equilibrium, and in the absence of other influences, the director will be perpendicular to any electric field. When filled with ZLI-4788-000, the PABN device is known to switch between its steady states [2], so we expect HAN cells filled with it to exhibit sign-dependent behaviour. One of the cell's glass walls was coated with Nissan 150 polyimide and rubbed, promoting planar homogeneous alignment, where the director is parallel to the surface and to the rubbing direction. A proprietary treatment supplied by Merck was used to promote homeotropic alignment at the other surface.

To study sign-dependent electro-optic effects, we applied a bipolar pulse, with potential difference

$$
v_0 = \begin{cases}
0, & t \leqslant 0, \\
+V, & 0 < t < \tau, \\
-V, & \tau \leqslant t < 2\tau, \\
0, & t \geqslant 2\tau,
\end{cases}
\tag{2}
$$

between the indium tin oxide electrodes. The time constant $\tau = 250$ ms is easily sufficient to allow the liquid crystal to reach equilibrium at each stage when driven by alternating fields; that is, when viscous dissipation determines the relaxation rate.

3. Numerical modelling

To model bipolar switching in a HAN cell, we find numerical solutions to the Ericksen–Leslie equations, with additional equations describing the motion of ionic impurities. The cell is far wider and broader (more than a centimetre) than it is deep ($3\,\mu$m), so we can neglect edge effects and treat the liquid crystal as uniform in the x- and y-directions, that is, varying only along the z-axis, normal to the cell substrates. We define the x-axis to be parallel to the rubbing direction on the planar surface. As a result, the director is everywhere parallel to the xz-plane, and so can be described solely by its tilt angle $\theta(z, t)$, measured from the z-axis in this paper. Incompressible flow is assumed, so the liquid crystal velocity vector has no z-component, and because all rotations of the director, and hence torques, are confined to the xz-plane, it has no y-component either. Inertial terms in the equations for the balance of linear and angular momenta are neglected, as they are assumed to relax on short timescales compared with re-alignment of the director [21].

Given these assumptions, the remaining state variables are the tilt $\theta(z, t)$, the x-component of the flow velocity $u(z, t)$ and the z-component of the electric field $E(z, t)$, together with the density, ρ_i, of each ion species (having charge q_i).

3.1. The Ericksen–Leslie equations

The z-component of the electric field is composed of two parts:

$$E = \frac{\sigma}{2\epsilon} - \frac{\partial v}{\partial z}. \tag{3}$$

The first term is due to the difference, σ, in surface charge density between the cell walls, while the second term is due to the applied field, ions in the bulk and the flexoelectric polarization. Since the first term contributes only a constant to the electric displacement, Gauss' law reduces to an equation in v,

$$\frac{\partial}{\partial z}\left(-\epsilon\frac{\partial v}{\partial z} + (e_s - e_b)\sin 2\theta \frac{\partial \theta}{\partial z}\right) = Q(z) = \sum_i q_i \rho_i. \tag{4}$$

The local permittivity ϵ is determined from the tilt angle, the ordinary dielectric constant $\epsilon_\perp$ and the dielectric anisotropy ϵ_a,

$$\epsilon = \epsilon_0\left(\epsilon_a \cos^2\theta + \epsilon_\perp\right). \tag{5}$$

Charged impurities in the bulk influence the electric field through the charge density, $Q(z)$, on the right-hand side of (4), and in turn affect the director profile, found by solving the equation for the conservation of angular momentum,

$$\left(k_{11}\sin^2\theta + k_{33}\cos^2\theta\right)\frac{\partial^2\theta}{\partial z^2} + \frac{1}{2}\left(k_{11} - k_{33}\right)\sin 2\theta \left(\frac{\partial\theta}{\partial z}\right)^2$$
$$+ \frac{1}{2}\sin 2\theta\left((e_s - e_b)\frac{\partial E}{\partial z} - \epsilon_0\epsilon_a E^2\right)$$
$$- (\alpha_3 - \alpha_2)\frac{\partial\theta}{\partial t} - (\alpha_3\sin^2\theta - \alpha_2\cos^2\theta)\frac{\partial u}{\partial z} = 0, \tag{6}$$

self-consistently with (4). Here, as usual, k_{11} and k_{33} are the splay- and bend-elastic constants, respectively.

Neglecting those terms proportional to the velocity gradient, $\partial u/\partial z$, in (6) would not alter the conclusions of this paper, but they are included in the model to show that the slow transients we encounter cannot be explained by their influence. To find the flow field, we solve the x-component of the conservation of linear momentum equation. Neglecting fluid inertia, we have

$$\frac{\partial}{\partial z}\left(h(\theta)\frac{\partial u}{\partial z} - (\alpha_3\sin^2\theta - \alpha_2\cos^2\theta)\frac{\partial\theta}{\partial t}\right) = 0, \tag{7}$$

where

$$h(\theta) = \tfrac{1}{2}[\alpha_4 + \alpha_5 + 2\alpha_3\sin^2\theta + \alpha_2(\sin^2\theta - \cos^2\theta)] + \alpha_1\cos^2\theta\sin^2\theta. \tag{8}$$

In equations (6)–(8), the six coefficients α_k are the Leslie viscosities, reduced to five by the Parodi relation $\alpha_6 - \alpha_5 = \alpha_2 + \alpha_3$. Only four independent linear combinations of the α_k affect switching in the HAN cell: $\alpha_3 - \alpha_2$, α_1, $\alpha_2 + \alpha_3$ and $\alpha_4 + \alpha_5$.

Equations (4), (6) and (7) must be solved together with appropriate boundary conditions. Strong anchoring at the cell walls, located at $z = 0$ and $z = d$, is assumed, so the boundary values $\theta(0, t) = 0$ and $\theta(d, t) = \pi/2$ do not change with time. Preliminary work showed that this assumption is reasonable, and even if weak anchoring is included in our models, it

Table 1. Values used for the material parameters of ZLI-4788-000.

Coefficient	Value
k_{11}	13.9 pN
k_{33}	21.1 pN
ϵ_a	−4.82
$\epsilon_\perp$	10.2
$\alpha_3 - \alpha_2$	365 mPa s
α_1	−10.0 mPa s
$\alpha_2 + \alpha_3$	−345 mPa s
$\alpha_4 + \alpha_5$	350 mPa s

does not substantially affect the slow transients we are interested in. The electric potential difference $v_0(t)$ is known, and since the model is unchanged by the addition of a constant to $v(z, t)$, we set $v(0, t) = v_0(t)$ and $v(d, t) = 0$. No-slip conditions are imposed on the flow: $u(0, t) = u(d, t) = 0$. Initial values $\theta(z, 0)$, $v(z, 0) = 0$ and $u(z, 0) = 0$ are given by the steady state solution to equations (4), (6) and (7) when no electric field is applied.

Numerical solutions to these equations can only be found if the many material parameters are known. Most of these, given in table 1, were found in an earlier study of the ac switching of the cell [22]. The remaining parameters, $(e_s - e_b)$ and σ were unknown before the experiment discussed here, indeed the original purpose of the experiment was to determine them. To this end, we optimize their values with respect to the optical measurements, subject to constraints that allow us to examine three models of sign dependence: one due to flexoelectricity, a second due to asymmetric surface charge distribution, and a third in which both mechanisms are important.

3.2. Ion drift-diffusion equations

To calculate the ion concentration (and hence the bulk charge density $Q(z)$), an hydrodynamic continuity equation,

$$\frac{\partial \rho_i}{\partial t} + \frac{\partial j_i}{\partial z} = 0, \tag{9}$$

must be solved, simultaneously with Gauss' law and the Ericksen–Leslie equations, for each ion species. The ion currents j_i are each made up of a diffusive contribution proportional to the density gradient, and a drift term proportional to the electric field:

$$j_i = -D_i \frac{\partial \rho_i}{\partial z} + \mu_i \frac{q_i}{|q_i|} \rho_i E. \tag{10}$$

The diffusivities D_i and mobilities μ_i are connected through the Einstein relation,

$$D_i = k_B T \mu_i / |q_i|. \tag{11}$$

Adsorption and desorption of charges at the cell walls are assumed to occur slowly over the timescale of the experiment, so isolating boundary conditions are imposed:

$$j_i(0, t) = j_i(1, t) = 0. \tag{12}$$

These boundary conditions do not specify a unique steady-state solution: the mean ion concentration ρ_{i0} must also be set for each species. Like $(e_s - e_b)$ and σ, the parameters μ_i and ρ_{i0} are unknown, and are varied to give the best match with experiment.

We have necessarily adopted a rather minimal model of ions in the cell. After all, there may be several impurity species, each with different mobilities, present in the liquid crystal. Some of these many species may well be adsorbed onto or desorbed from the cell walls over the timescale of the experiment. However, we can assume that at least one species remains stuck to the walls for longer periods or there would be no equilibrium sign-dependent effect due to them, as there appears to be.

3.3. Numerical method

Equations (4), (6), (7) and (9) must, in general, be solved numerically. We used the control volume method [23], dividing the liquid crystal layer into 48 uniformly sized sub-layers, and integrating the governing equations over each. The backward Euler formula is then used to integrate the resulting ordinary differential equations over time, leading to a set of nonlinear algebraic equations. Each of these relates the values of v, θ, u and the ρ_i at the centres of a given sub-layer and at a given time step, to the values in the adjacent sub-layers at the current time step, and to the value in the same layer at the previous time-step. These equations are solved at each time step by a quasi-Newton method. Starting from either a steady-state solution or values at the previous time step, v, θ, u and then the ρ_i are updated in turn until their values converge. For example, the update to the tilt profile, θ, is calculated by assuming values for all the other variables, and then linearizing the resulting set of equations to find a Newton step $\delta\theta$. The time steps are chosen adaptively, such that the result of taking one step of length Δt and two steps of length $\Delta t/2$ differ by less than some chosen tolerance.

The precise relationship between, say, θ in the centre of one sub-layer and θ in the centre of the neighbouring sub-layers depends upon the gradient of θ at the adjoining faces. Although the gradients of θ, u and v can be safely approximated by the central difference formula, ρ_i must be treated with more care. When an electric field is applied, strong gradients in ρ_i occur near the cell walls, and use of the central difference formula would result in unphysical negative values unless the sub-layers were very fine. This problem is avoided if ρ_i is assumed to vary exponentially from the centre of one sub-layer to the next.

This numerical recipe was implemented in a C++ function, which can be driven through GNU R. It is freely available for both use and modification; at the time of writing it can be obtained from http://r-forge.r-project.org/projects/photonics/.

4. Results

While the steady-state results are well described by the Ericksen–Leslie equations without the ion diffusion equations, the time-dependent behaviour of the cell is not [13]. The observed mid-plane tilt is plotted as a function of time in figure 2 for several values of V. All the curves tend to equilibrium values that depend upon both the magnitude and the sign of the applied voltage. They also exhibit several transient features which occur over timescales that shrink as the magnitude of the applied voltage grows. In comparison, mid-plane tilts found by solving the Ericksen–Leslie equations alone (including the flexoelectric effect but not ions) are plotted in figure 3. The equilibrium values are similar to those observed experimentally, but there
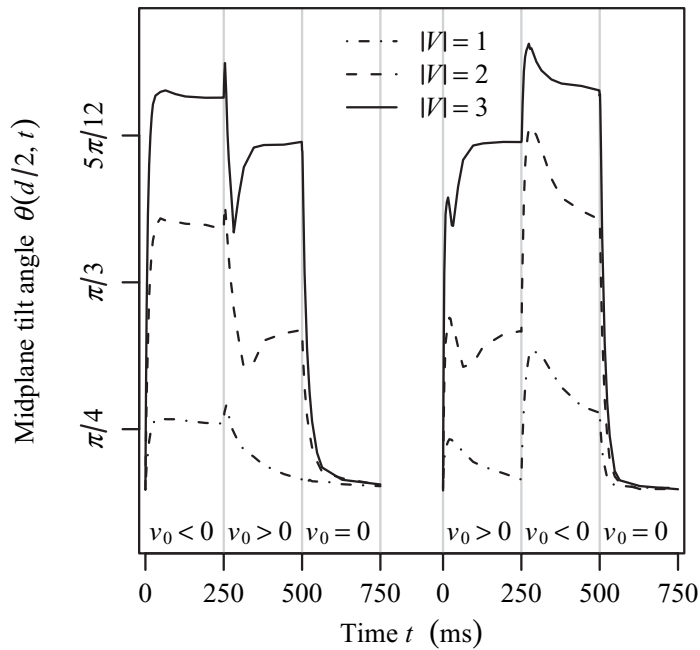
Figure 2. Observed evolution of the mid-plane tilt. In addition to the difference between equilibrium states at $v_0 > 0$ and $v_0 < 0$, transient behaviour not explained by the Ericksen–Leslie equations alone is apparent. In particular, there is a dip in the mid-plane tilt shortly after the cell is switched to a positive voltage, whatever its previous state.
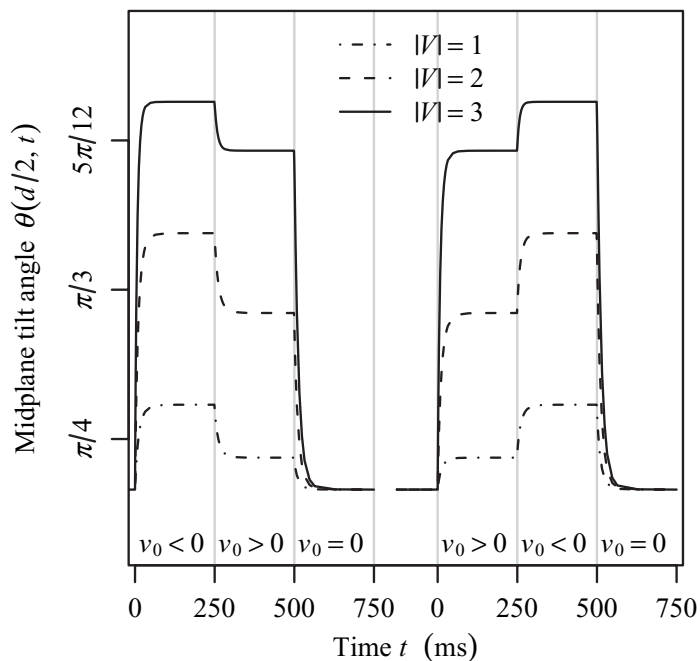

Figure 3. Modelled evolution of the mid-plane tilt with no ions present. Sign dependence is due to the flexoelectric effect, with $(e_s - e_b) = 30\,\mathrm{pC\,m^{-1}}$. Although the equilibrium states are in agreement with the observations in figure 2, the large amplitude transients are missing entirely.
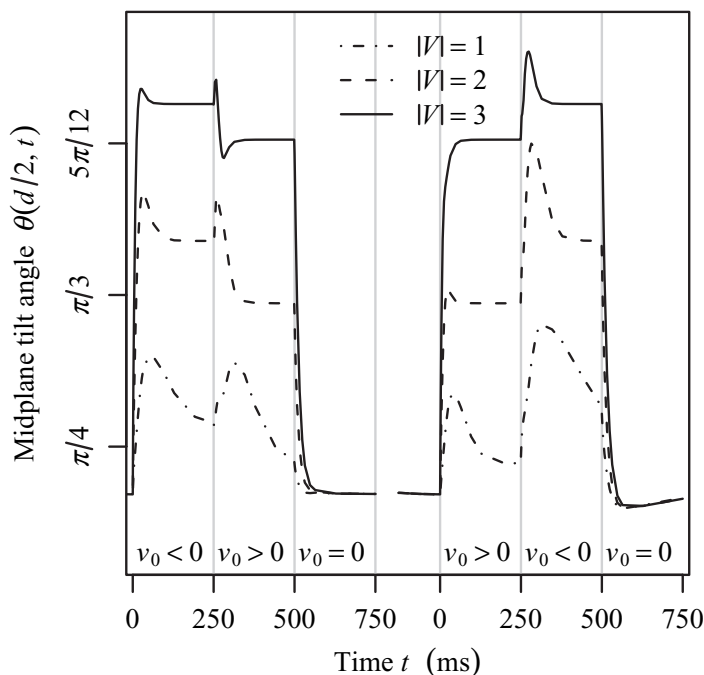
Figure 4. Modelled evolution of the mid-plane tilt when the sign-dependent effect is dominated by flexoelectricity, with $(e_s - e_b) = 22\,\text{pC}\,\text{m}^{-1}$. In contrast to the observations (figure 2), the time-dependent behaviour immediately after the cell is switched from $v_0 = 0$ to $v_0 > 0$ does not resemble that when the cell is switched from $v_0 < 0$ to $v_0 > 0$.

are no significant transients. In fact, the timescales of the transients—around 100 ms, are far longer than the ~10 ms timescales seen in the ac switching of the same cell [22], where ion motion is negligible, and so we should not expect to find them when modelling the dc switching this way.

All of the transients observed occur immediately after the applied voltage is changed, and over a timescale of around 100 ms. When the polarity of the applied field is switched from $v_0 > 0$ to $v_0 < 0$, the director initially rotates beyond the $v_0 < 0$ steady state, as though the field was supplemented for a short period. Another pair of transients suggest that the ground state of the cell and the $v_0 < 0$ steady-state are similar to each other and distinct from the $v_0 > 0$ steady-state: a few milliseconds after the field is switched from negative to positive *and* from off to positive, the director rotates away from the $v_0 > 0$ steady state towards the ground state, then back towards the $v_0 > 0$ steady state, resulting in a distinctive dip in plots of the mid-plane tilt against time.

To explain these transients, we included two species of mobile ions in our models, one having charge $-e$, that is, the charge on an electron, and the other having charge $+e$. Their mean densities were set to $\rho_{0-} \approx 1.5 \times 10^{20}\,\text{m}^{-3}$ and $\rho_{0+} \approx 3 \times 10^{20}\,\text{m}^{-3}$ and their mobilities to $\mu_- \approx 3.0 \times 10^{-10}\,\text{m}^2\,\text{V}^{-1}\,\text{s}^{-1}$ and $\mu_+ \approx 1.5 \times 10^{-10}\,\text{m}^2\,\text{V}^{-1}\,\text{s}^{-1}$. Similar values have been reported elsewhere [17, 24]. The exact values vary slightly in the results that follow since they are chosen to best fit the data. These mobile ions cause transients to be calculated with the correct amplitudes and timescales in all of the models, but the details depend noticeably on the sign-dependent mechanism.
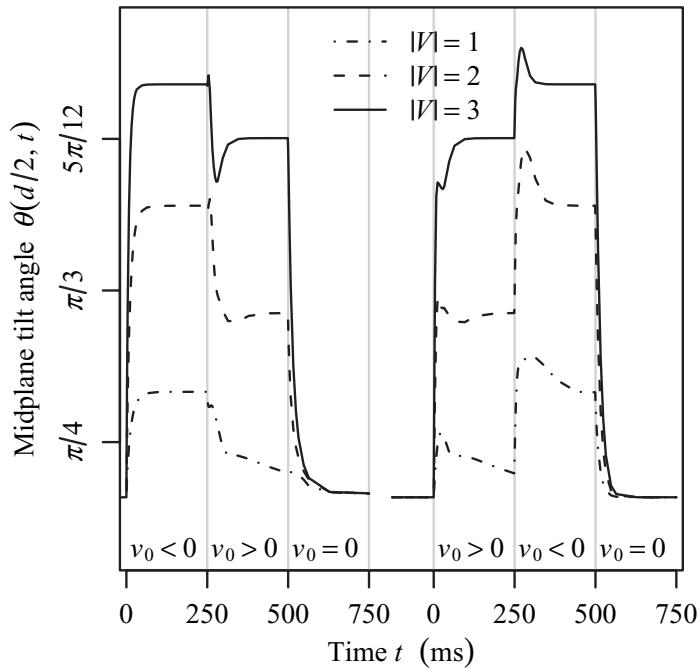
Figure 5. Modelled evolution of the mid-plane tilt when the sign-dependent effect is dominated by surface charges ($\sigma = 14\,\mu\mathrm{C\,m}^{-2}$). In this case, the director evolves in a similar manner when the cell is switched from $v_0 = 0$ to $v_0 > 0$ and when it is switched from $v_0 < 0$ to $v_0 > 0$, as in the observations (figure 2).

Sign-dependent behaviour in the first numerical model, shown in figure 4, is due to the flexoelectric effect, with $(e_s - e_b) = 22\,\mathrm{pC\,m}^{-1}$. While the director behaves in the correct manner when the cell is switched from $v_0 > 0$ to $v_0 < 0$, at several other points it does not. Shortly after the switch from $v_0 = 0$ to $v_0 < 0$, the director briefly rotates beyond the steady-state position by an angle which increases as $|v_0|$ decreases. While an over-rotation is observed experimentally, it is weak and decreases in amplitude as $|v_0|$ decreases. A dip in the mid-plane tilt is calculated after the switch from $v_0 < 0$ to $v_0 > 0$ only when $|v_0| = 3$, and not at all after the switch from $v_0 = 0$ to $v_0 > 0$. Finally, when the field is switched from $v_0 > 0$ to $v_0 = 0$, the director rotates beyond the ground state and then back.

If surface charges, with $\sigma = 14\,\mu\mathrm{C\,m}^{-2}$, are assumed to dominate over the flexoelectric effect, the numerical results, shown in figure 5, resemble the observations rather more closely. As in the previous case, the director rotates beyond the equilibrium state when the cell is switched from $v_0 > 0$ to $v_0 < 0$. But, unlike the previous case, and in common with the experimental results, a dip in the mid-plane tilt is present both at switch-on to $v_0 > 0$ and at the switch from $v_0 < 0$ to $v_0 > 0$. There is one qualitative difference between these calculations and the experiment—no over-rotation is seen as the cell evolves from the ground state towards the $v_0 < 0$ steady state. This might be explained if additional, slower moving ion species were considered.

The underlying difference between these two cases, at least in terms of the ion dynamics, is in their ground state charge distributions, and this is reflected in the transient behaviour of the director. Figure 6 shows that when surface charge is the primary sign-dependent
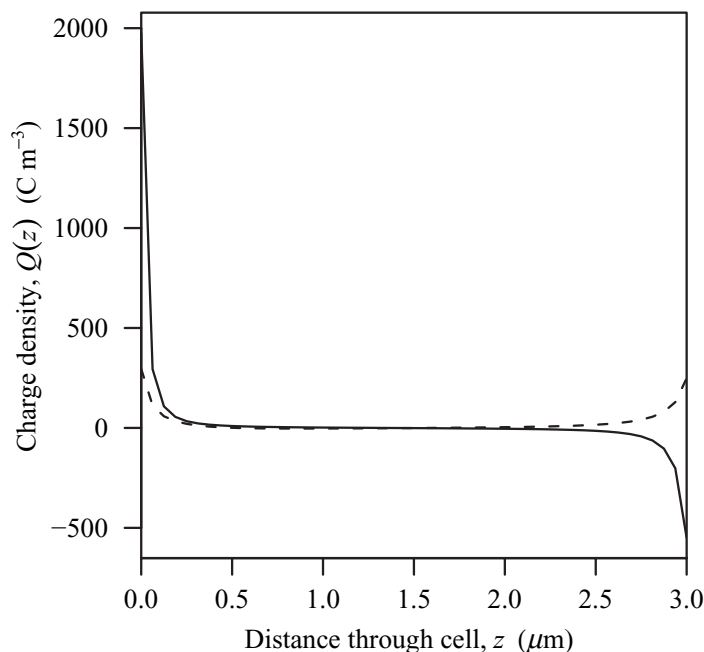
Figure 6. Modelled charge distribution in the ground state. When sign dependence is due to surface charges, the ground state charge distribution (solid curve) is highly asymmetric, with positive ions concentrated near the homeotropic surface (at $z = 0$), much as they would be if a negative voltage were applied. When flexoelectricity is more important (dashed curve), ions are distributed much more evenly.

mechanism, positive charge is strongly concentrated near the homeotropic wall at $z = 0$. A similar concentration will occur if a negative voltage is applied. As a result, whenever a positive voltage is applied, whether the cell is initially in the ground state or the $v_0 > 0$ steady state, a similar migration of positive ions to the opposite wall is expected. For a short period, there is an even distribution of charge across the cell, and it is during these periods that the distinctive dips in the tilt profile occur. In other words, the dip is calculated only if the initial charge distribution is higher at one wall, and that occurs at two times for this model: when the cell is switched on to a positive voltage, and when it is switched from a negative to a positive voltage.

On the other hand, when the flexoelectric effect is the cause of sign dependence, positive charge is not concentrated near the homeotropic wall. In this case, the ground state charge distribution—the dashed curve in figure 6—is nearly uniform[3]. Only when the cell is switched from a negative to a positive voltage is a dip in the tilt profile computed.

A best-fit model (figure 7), where the parameters $(e_s - e_b) = -7\,\mathrm{pC\,m^{-1}}$ and $\sigma = 17\,\mu\mathrm{C\,m^{-2}}$ are chosen to minimize the difference between the observed optical data and the model, is similar to the surface-charge dominated model. Notably, the flexoelectric polarization is small, and directed in the opposite sense to the flexoelectric polarization in the first model.

---

[3]   The modest rise in charge density at both surfaces happens because there is an excess of positive charge in the bulk: if there is no excess, the distribution is nearly uniform. The transient behaviour of the liquid crystal is hardly affected by this.
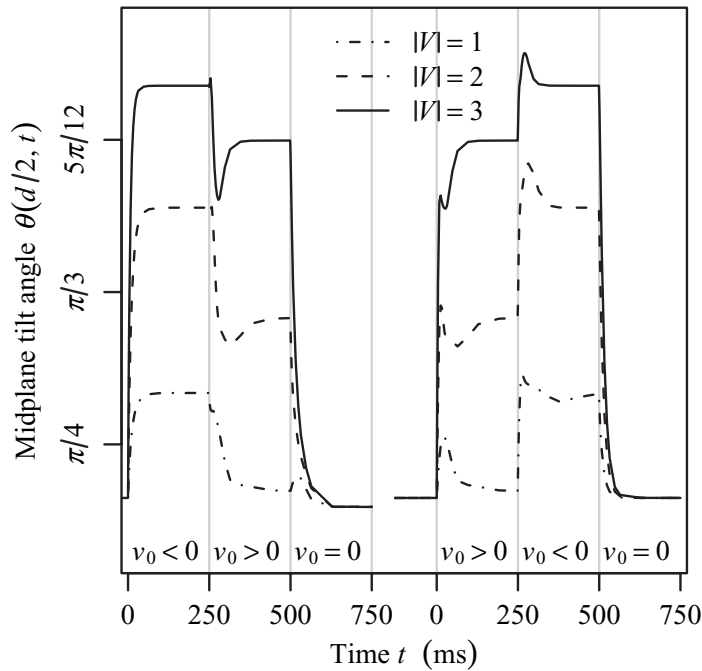
Figure 7. Modelled evolution of the mid-plane tilt in the best fit case ($(e_s - e_b) = -7\,\text{pC}\,\text{m}^{-1}$, $\sigma = 16\,\mu\text{C}\,\text{m}^{-2}$). As in the previous case (figure 5), the transient features are consistent with those in the observations (figure 2).

5. Conclusions

We observed both sign-dependent equilibria and slow transients during the bipolar switching of a HAN cell filled with Merck ZLI-4788-000. The slow transients cannot be caused by ordinary nematodynamic phenomena, because their amplitude is too large, and their timescale too long. They are, however, consistent with a drift-diffusion model of ion motion, since their timescales shrink as the applied voltage grows. The concentration of ionic impurities appears to be tiny—around $10^{20}\,\text{m}^{-3}$, but nonetheless strongly affects dc switching.

Experimentally, when a positive potential was applied across the electrodes of a cell in the ground state, the director did not evolve monotonically towards an excited state. Rather, a temporary rotation towards the ground state was observed, as a dip in a plot of mid-plane tilt against time, shortly after a voltage was applied. A similar dip occurred when the cell was switched from a negative to a positive voltage. Numerical modelling predicts these temporary rotations, which occur when positive charge migrates from the homeotropic surface to the planar surface, only if the homeotropic wall is negatively charged. In contrast, if the flexoelectric effect is assumed to account for the sign dependence, the initial ion concentration is uniform across the cell in the ground state, and the director should rotate monotonically towards both positive and negative steady states. For ZLI-4788-000, then, the coefficient $(e_s - e_b)$ is small, and the influence of the flexoelectric effect on dc switching in a HAN cell is less important than that due to ionic impurities.

IOP Institute of Physics ⦿ DEUTSCHE PHYSIKALISCHE GESELLSCHAFT

References

 [1] Bryan-Brown G P, Brown C V, Jones J C, Wood E L, Sage I C, Brett P and Rudin J 1997 *SID Dig.* **28** 37
 [2] Kitson S and Geisow A 2002 *Appl. Phys. Lett.* **80** 3635
 [3] Meyer R B 1969 *Phys. Rev. Lett.* **22** 918
 [4] Rudquist P and Lagerwall S T 1997 *Liq. Cryst.* **23** 503
 [5] Takahashi T, Hashidate S, Nishijou H, Usui M, Kimura M and Akahane T 1998 *Japan. J. Appl. Phys.* **37** 1865
 [6] Mazzulla A, Cuichi F and Sambles J R 2001 *Phys. Rev.* E **64** 021708
 [7] Jewell S A and Sambles J R 2002 *J. Appl. Phys.* **92** 19
 [8] Warrier S R and Madhusudana N V 1997 *J. Physique* **7** 1789
 [9] Davidson A J and Mottram N J 2002 *Phys. Rev.* E **65** 051710
[10] Barbero G, Evangelista L R and Olivero D 2000 *J. Appl. Phys.* **87** 2646
[11] Barbero G, Zvezdin A K and Evangelista L R 1999 *Phys. Rev.* E **59** 1846
[12] Evangelista L R and Barbero G 2006 *Liq. Cryst.* **33** 1
[13] Taphouse T S, Cornford S L, Birkett J E and Sambles J R 2008 *New J. Phys.* **10** 083045
[14] Stewart I W 2004 *The Static and Dynamic Continuum Theory of Liquid Crystals* (London: Taylor and Francis)
[15] Leslie F M 1968 *Arch. Ration. Mech. Anal.* **28** 265
[16] Evangelista L R and Barbero G 2004 *Liq. Cryst.* **31** 1399
[17] Smith A A T, Brown C V and Mottram N J 2007 *Phys. Rev.* E **57** 041704
[18] Jewell S A, Taphouse T S and Sambles J R 2005 *Appl. Phys. Lett.* **87** 0201106
[19] Fuzi Y and Sambles J R 1999 *J. Opt. Soc. Am.* B **16** 288
[20] Berreman D W 1972 *J. Opt. Soc. Am.* **62** 502
[21] van Doorn C V 1975 *J. Appl. Phys.* **46** 3738
[22] Cornford S L, Taphouse T S, Newton C J P and Sambles J R 2007 *New J. Phys.* **9** 166
[23] Patankar S V 1980 *Numerical Heat Transfer and Fluid Flow* (London: Taylor and Francis)
[24] Neyts K, Vermael S, Desimpel C, Stojmenovik G, Vershueren A R M, de Boer D K G, Snijkers R, Machiels P and van Brandenburg A 2003 *J. Appl. Phys.* **94** 3891
[25] R Development Core Team 2008 *R: A Language and Environment for Statistical Computing* (Vienna: R Foundation for Statistical Computing)